Available online at www.sciencedirect.com
SCIENCE DIRECT®

Catalysis Today 90 (2004) 313–317

CATALYSIS TODAY

www.elsevier.com/locate/cattod

Photocatalytic reduction of water by TaON under visible light irradiation

Michikazu Hara[a], Tsuyoshi Takata[a], Junko N. Kondo[a], Kazunari Domen[a,b,*]

[a] Chemical Resources Laboratory, Tokyo Institute of Technology, 4259 Nagatsuta, Midori-ku, Yokohama 226-8503, Japan
[b] Core Research for Evolutional Science and Technology, Japan Science and Technology Co. (CREST, JST),
2-1-13 Higashi-ueno, Daito-ku 110-0015, Japan

Abstract

Some noble metals have been studied as H_2 evolution promoters for TaON, a visible light driven oxynitride photocatalyst. H_2 evolution on TaON photocatalyst under visible light irradiation ($420\,\text{nm} \leq \lambda \leq 500\,\text{nm}$) in an aqueous methanol solution was found to be remarkably enhanced by adding Ru as a noble metal co-catalyst.

Keywords: Photocatalyst; Oxynitride; Visible light

---

1. Introduction

In order to satisfy energy conservation requirements and the increasingly stringent standards of environmental regulations, catalytic techniques are being applied in various fields. Photocatalysis is one technique that has great potential for the conversion of photon energy into chemical energy and to decompose pollutants in air or solution. Any photocatalyst that functions in visible light would have genuine applications in solar energy utilization.

Photocatalysts that function in the visible region ($400\,\text{nm} < \lambda < 800\,\text{nm}$) are desirable from the viewpoint of solar energy utilization. Recently, Asahi et al. have reported nitrogen-doped TiO_2 as a visible light driven photocatalyst for organic material degradation in air [1] and Arakawa and co-workers found that photocatalytic overall water splitting proceeds over $InTaO_4$ under visible light irradiation [2]. Recently, the present authors have reported several stable non-oxide photocatalysts as potential candidates for visible light-induced overall water splitting [3–7]. (Oxy)nitrides such as Ta_3N_5, TaON and $LaTiO_2N$ have significant absorption in the visible light region, with absorption edges at 500–600 nm corresponding to bandgap energies of 2.0–2.5 eV. By these bandgap excitations, these (oxy)nitrides function as photocatalysts for H_2 or O_2 evolution from aqueous solutions containing a sacrificial electron donor (methanol) or acceptor (Ag^+), with potential for overall water splitting. Among these catalysts, TaON, which has a bandgap of 2.5 eV (absorption edge at 500 nm), has conduction and valence band edges of ca. -0.3 and $+2.2$ V versus NHE ($pH = 0$), respectively, sufficient for splitting water into H_2 and O_2. TaON exhibits particularly high photocatalytic activity for the oxidation of water, with quantum efficiency for O_2 evolution at 420–500 nm of ca. 30%. However, the quantum efficiency for H_2 evolution from an aqueous methanol solution on Pt-loaded TaON is only about 0.2%. To accomplish overall water splitting under visible light irradiation using this catalyst, it is necessary to develop a modification method to facilitate H_2 evolution. In this letter, several noble metals (Pt, Ru, Rh, and Ir), included as additive metal complexes in the reaction solution, are examined as potential H_2 evolution promoters.

2. Experimental

TaON was prepared by heating Ta_2O_5 powder (Rare Metallic Co., Ltd., purity 99.9%) in a quartz tube reactor under flowing NH_3 gas containing water vapor at 1123 K for 10 h. A mixture of NH_3 gas ($100\,\text{mL}\,\text{min}^{-1}$) and N_2

---

[*] Corresponding author. Tel.: +81-45-924-5238; fax: +81-45-924-5282.
E-mail address: kdomen@res.titech.ac.jp (K. Domen).

0920-5861/$ – see front matter © 2004 Elsevier B.V. All rights reserved.
doi:10.1016/j.cattod.2004.04.040

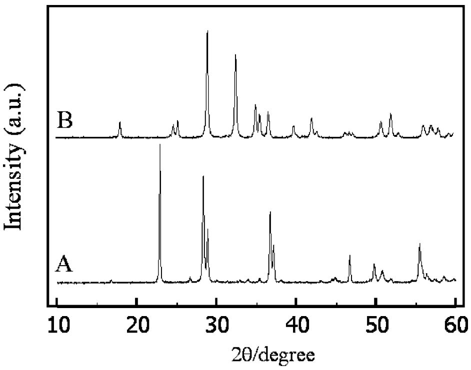

Fig. 1. XRD patterns of (A) Ta_2O_5 and (B) TaON.

gas (1 mL min^{-1}) bubbled through water at 283 K was introduced into the quartz reactor. The flow rate of water was estimated to 12 μL min^{-1}. Without the presence of water vapor, nitridation resulted in significant production of Ta_3N_5 as a byproduct, lowering the photocatalytic activity. In contrast, the introduction of large amounts of water vapor prevented nitridation of Ta_2O_5. Fig. 1 shows X-ray powder diffraction patterns of TaON and Ta_2O_5. The XRD pattern for TaON corresponds to that of β-TaON in the literature [8]. UV-Vis diffuse reflectance spectra of TaON and Ta_2O_5 are shown in Fig. 2. The absorption band-edge of TaON is ca. 500 nm, being shifted by about 170 nm from that of Ta_2O_5, and the bandgap energy was estimated to be 2.5 eV. Elemental analysis revealed that the composition of the sample was $TaO_{1.24}N_{0.84}$, indicating that the prepared “TaON” was non-stoichiometric and defective.

The reaction was carried out in a Pyrex reaction vessel connected to a closed glass gas circulation system. H_2 evolution was examined in 200 mL aqueous solutions containing 0.40 g TaON, 160 mL methanol or ethanol as a sacrificial electron donor, and 2×10^{-7} to 4×10^{-4} mol H_2PtCl_6, $(NH_4)_2IrCl_6$, $(NH_4)_2RhCl_6$ or $(NH_4)_2RuCl_6$. The reaction solution was evacuated several times to purge air, followed by irradiation with a 300 W Xe lamp equipped with a cut-off filter ($\lambda \geq 420$ nm). It is well known that such complexes are reduced into metal particles on bandgap-excited photocatalysts and they function as H_2 evolution promoter. The evolved gas was analyzed by gas chromatography. For comparison, Pt- and Ru-loaded TaON were prepared by the following impregnation method. TaON was impregnated with noble metal chloride complexes, and the complexes on TaON were reduced into metal particles by heating at 473 K in H_2 (2.6×10^4 Pa) for 5 h. The H_2 evolutions on Pt- and Ru-loaded TaON were also examined in a similar manner as above.

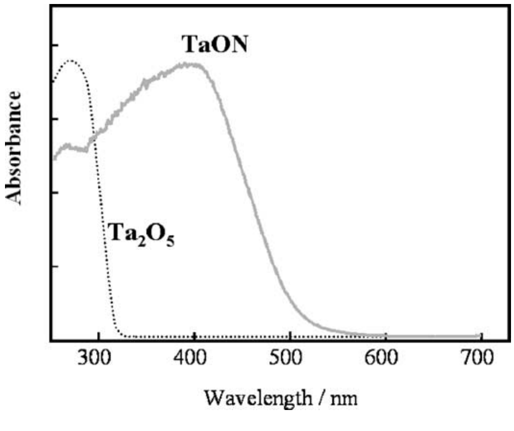

Fig. 2. UV-Vis diffuse reflectance spectra of TaON and Ta_2O_5.

Quantum efficiencies (Φ) were calculated using the following equation: $\Phi(\%) = (AR/I) \times 100$, where A represents the coefficient based on the reaction (for H_2 evolution: 1), R represents the H_2 evolution rate (molecules h^{-1}), and I represents the rate of absorption of incident photons. The number of photons reaching the solution was measured with a Si photo-diode, and the rate of total incident photons at 420 nm $\leq \lambda \leq$ 500 nm was typically 9.6×10^{21} photons h^{-1}. We assumed that visible light at $\lambda \leq$ 500 nm was available for the photoreactions because TaON did not work at $\lambda <$ 500 nm, and that all incident photons are absorbed by the suspension ($I = 9.6 \times 10^{21}$ photons h^{-1}). Therefore, calculated Φ is the apparent quantum efficiency.

The surface areas of Ru and Pt particles on TaON were obtained by measuring H_2 adsorption isotherm for each sample in a small Pyrex cell connected to a small closed glass system (total dead volume: 20.5 cm^3). By H_2 adsorption on 0.05 wt.% Ru- and Pt-TaON at 290 K, Langmuir adsorption isotherms were obtained, and the surface areas of Ru and Pt particles were estimated from saturated adsorbed amounts of H_2 at the temperature because it was confirmed that TaON itself does not adsorb H_2. When spherical or hemispherical metal particles are deposited on TaON, the particle size r is given by the following equation: $r = 6A/S\rho$, where A represents the total weight of metal particles (2×10^{-4} g), S represents the total surface area of metal particles (m^2), and ρ represents the density of metal (g m^{-3}).

3. Results and discussion

Fig. 3 shows the variation in H_2 evolution rate with different amounts of the various noble metals introduced as metal complexes in the reaction solutions. Inductively coupled plasma mass spectrometry confirmed that the solution contained no remnant noble metal complexes after all reactions. In XPS for TaON samples after reactions, the peaks due to Ta^{5+}, O, N and metallic noble metals were observed, but there was no peak assigned to oxidize noble metals. These results indicate that all metal complexes in the solutions were reduced to metal particles. The rate of H_2 evolution was measured after 1 h. Simultaneous evolution of CO_2 due to oxidation of methanol was also confirmed, and neither N_2 nor O_2 were evolved during reaction. Although the tested noble metals are generally excellent catalysts for H_2 evolution on oxide photocatalysts such as TiO_2, the rates of H_2

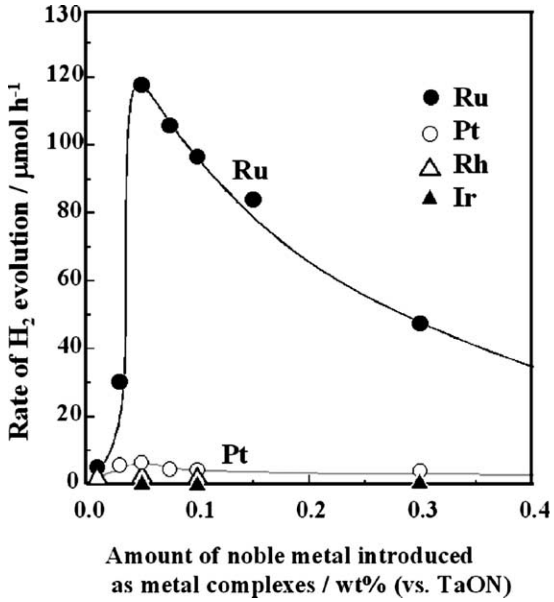

Fig. 3. Dependence of H_2 evolution rate on the amount of metal introduced as metal complexes (TaON 0.4 g, 80 vol.% methanol solution 200 mL).

evolution for Pt-, Ir- and Rh-TaON were only 2–8 μmol h^{-1} (quantum efficiency of 0.01–0.05%) even under optimum conditions (ca. 0.05 wt.% loading). In the case of Ru-TaON, the rate of H_2 evolution increased with the amount of added Ru, reaching a maximum (ca. 120 μmol h^{-1}) at 0.05 wt.%. Further addition of Ru beyond 0.05 wt.% lowered the activity, as shown in Fig. 3. Time courses of H_2 evolution on 0.05 wt.% Ru-TaON in aqueous methanol and ethanol solutions are shown in Fig. 4. The quantum efficiencies for H_2 evolution on 0.05 wt.% in aqueous methanol and ethanol solutions were estimated to be 0.8 and 2.1%, respectively.

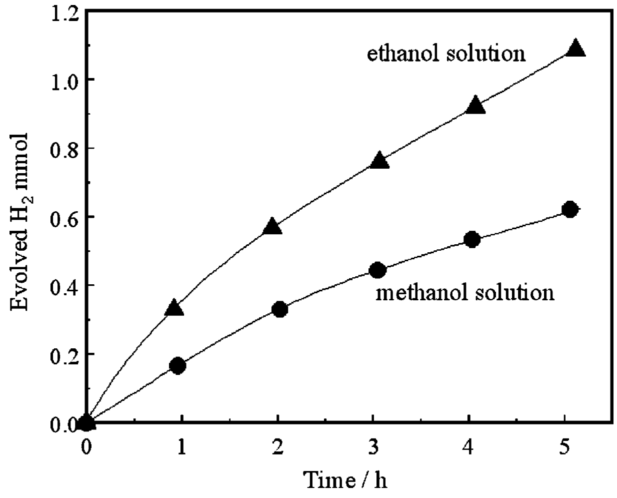

Fig. 4. Time courses of H_2 evolution on 0.05 wt.% Ru-TaON in aqueous methanol and ethanol solutions under visible light irradiation ($\lambda \geq 420$ nm). TaON: 0.4 g, 80 vol.% methanol or ethanol solution: 200 mL.

In Pt- and Ru-loaded TaON prepared by impregnation, Pt was the more effective promoter for H_2 evolution. Even under optimum loaded amounts, however, the quantum efficiencies for H_2 evolution in an aqueous methanol solution on Ru-loaded TaON (Ru 5 wt.%) and Pt-loaded TaON (Pt 3 wt.%) prepared by impregnation were 0.1 and 0.2%, respectively, much lower than in the present case. Fig. 5 shows SEM images of 0.05 wt.% Ru-photodeposited TaON and 5 wt.% Ru-loaded TaON (impregnation method), suggesting that the difference between both samples in activity is attributed at least in part to the difference in particle sizes, 20–50 nm by impregnation and 2–4 nm by the present method.

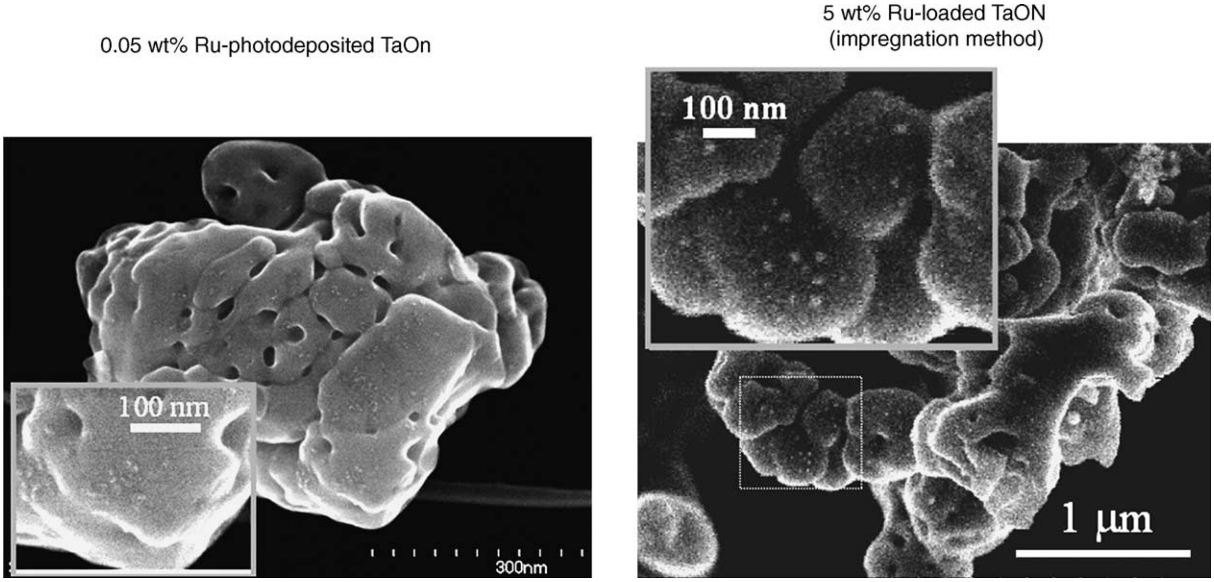
0.05 wt% Ru-photodeposited TaOn

5 wt% Ru-loaded TaON
(impregnation method)

Fig. 5. SEM images of 0.05 wt.% Ru-TaON (photodeposition) and Ru-loaded TaON (Ru 5 wt.%: impregnation method).

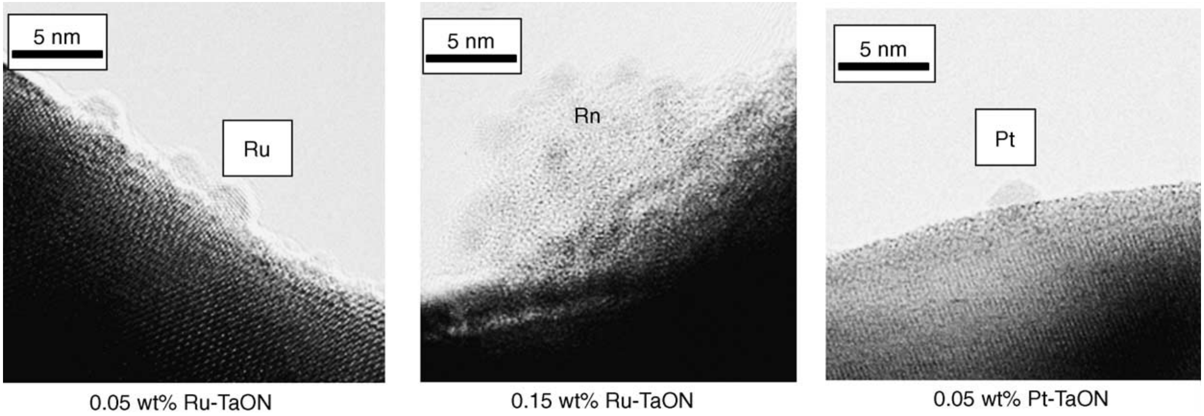

Fig. 6. TEM images of Ru- and Pt-TaON.

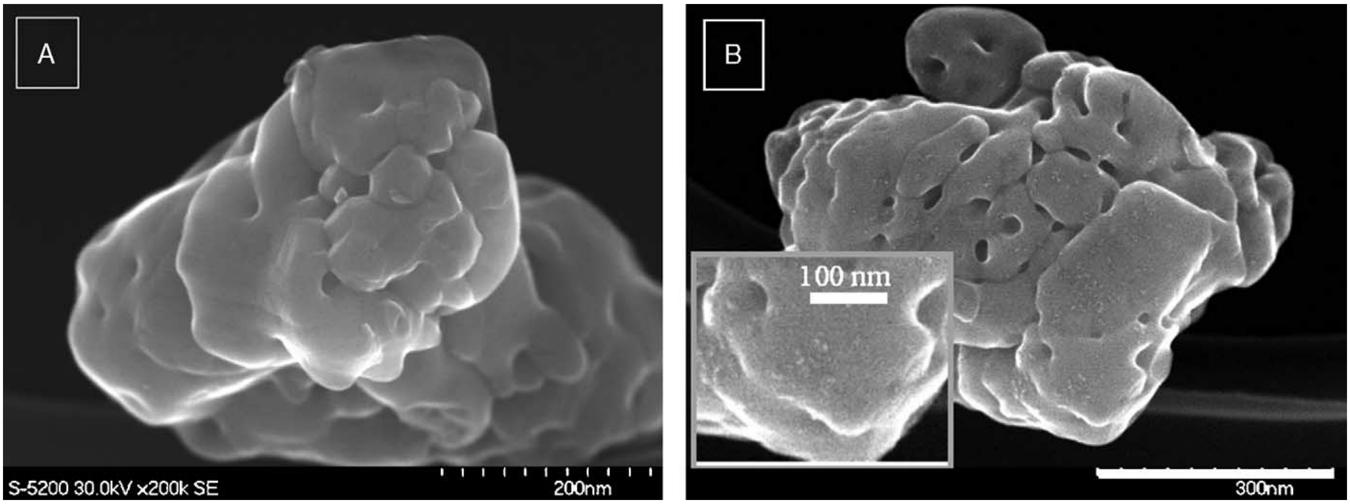

Fig. 7. SEM images of 0.05 wt.% Ru-TaON.

In the tested noble metals, Pt has a particularly low activation overpotential for H_2 evolution[1] and this is consistent with the fact that Pt exhibits the highest H_2 evolution activity in metal hydrogen evolution promoters on metal oxide photocatalysts [10]. As a result, the remarkable performance of Ru-TaON cannot be attributed to overpotential or H_2 evolution activity. To investigate this further, the morphology and dispersion of deposited metal particles were examined by transmission electron microscopy (TEM). TEM images of Ru- and Pt-TaON are shown in Fig. 6. Metallic Ru particles of 2–4 nm were dispersed on 0.05 wt.% Ru-TaON, whereas on 0.15 wt.% Ru-TaON, the Ru particles tended to aggregate, with a negative impact on the rate of H_2 evolution. In the TEM image of 0.05 wt.% Pt-TaON, a Pt particle of ca. 4 nm was observed. To compare the surface area of Ru particles with that of Pt particles, H_2 adsorption isotherms for both samples were measured. Assuming that a noble metal atom on the particle surfaces adsorbs a hydrogen atom, the surface areas of Ru and Pt particles on 0.4 g of 0.05 wt.% Ru- and Pt-TaON were estimated to be 1.2×10^{-7} and $1.4 \times 10^{-7}\,\mathrm{m}^2$, respectively. When spherical or hemispherical noble metal particles were deposited on TaON, the particle sizes of Ru and Pt calculated on the basis of the surface areas were ca. 8 and 4 nm, respectively. As a result, there is no considerable difference in surface area and particle size between Ru and Pt particles on TaON, and the high H_2 evolution activity of Ru-TaON cannot be attributed to morphology. Instead, the interface electronic structure between Ru particles and TaON may be responsible, possibly facilitating electron transfer from TaON to Ru. Pt particles may not be able to act as an efficient electron transfer mediator due to poor electronic contact with the TaON. To the best of the authors' knowledge, such behavior has not been observed on oxide photocatalysts. More detailed study is therefore necessary to determine how these electronic mechanisms differ from conventional oxide photocatalysts.

It should be noted that TaON has no large amount of effective sites for photoreduction. Fig. 7 shows high resolution

---

[1] The activation overpotential (η) for reduction of H^+ to H_2 is given by $\eta = b \ln i_0 - b \ln i$; where b, i_0 and i represent the Tafel slope (mV), exchange current density ($\mathrm{A\,cm^{-2}}$) and current density ($\mathrm{A\,cm^{-2}}$). For 0.5–1.0 M H_2SO_4 solution, the Tafel slopes of Ru, Pt, Ir and Rh are 120, 25, 122 and 120 mV, and $\ln i_0$ values are −2.1, −3.1, −2.8 and −1.9 [9].

SEM images of 0.05 wt.% Ru-TaON. Ru particles were not observed on most of 0.05 wt.% Ru-TaON particles (>90%) as shown in Fig. 7A. TaON particles with observable Ru particles was only 10–20% of the whole (Fig. 7B). Apparently, most of TaON particles do not function for photoreduction although the conduction band has a sufficient potential to reduce $(NH_4)_2RuCl_6$ and H^+ into H_2 efficiently [7]. This suggests that in TaON excited electrons are not efficiently available for photoreduction process.

4. Conclusions

The addition of Ru to the reaction solution as an additive metal complex in the reduction of water under visible light using a TaON photocatalyst was found to promote the evolution of H_2. Other noble metals, Pt, Ir and Rh, added under identical conditions were not as effective.

Acknowledgements

This work was supported by the Core Research for Evolutional Science and Technology (CREST) program of the Japan Science and Technology Corporation (JST) and The 21st Century Center of Excellence (COE) program of the Ministry of Education, Science, Sports and Culture of Japan.

References

[1] R. Asahi, T. Morikawa, T. Ohwaki, K. Aoki, Y. Taga, Science 293 (2001) 269.
[2] Z. Zou, J. Ye, K. Sayama, H. Arakawa, Nature 414 (2001) 625.
[3] G. Hitoki, A. Ishikawa, T. Takata, J.N. Kondo, M. Hara, K. Domen, Chem. Lett. (2002) 736.
[4] G. Hitoki, T. Takata, J.N. Kondo, M. Hara, H. Kobayashi, K. Domen, Chem. Commun. (2002) 1968.
[5] A. Kasahara, K. Mukumizu, G. Hitoki, T. Takata, J.N. Kondo, M. Hara, H. Kobayashi, K. Domen, J. Phys. Chem. A 106 (2002) 6750.
[6] A. Kasahara, K. Mukumizu, G. Hitoki, T. Takata, J.N. Kondo, M. Hara, H. Kobayashi, K. Domen, J. Phys. Chem. B 107 (2003) 791.
[7] W.-A. Chun, A. Ishikawa, H. Fujisawa, T. Takata, J.N. Kondo, M. Hara, M. Kawai, Y. Matsumoto, K. Domen, J. Phys. Chem. B 107 (2003) 1798.
[8] B. Armytage, B.E.F. Fender, Acta Crystallogr. B 30 (1974) 809.
[9] A.J. Bard (Ed.), Encyclopedia of Electrochemistry of the Elements, vol. IXa, Marcel Dekker, p. 383.
[10] H. Kanno, Y. Yamamoto, H. Harada, Chem. Phys. Lett. 121 (1985) 245.